

RANDOM WALK SOURCE MODEL AND C_f

Ronald Meyer

Presented at the XXVI OSTIV Congress, Bayreuth, Germany

ABSTRACT

The author extends his numerical method for obtaining the lift coefficient of wing sections which bases on a random walk algorithm. In the former paper [2] the phenomenon of migrating fluid fronts in filter paper around macroscopic obstacles lead to a numerical model of unsteady potential flow the author calls "random walk source model." The shape of the migrating fluid fronts simulated in the random walk model tells the history of the path of fluid particles on their way them to the front; it thus carries the information about the lift coefficient of the passed wing section. He now studies the path of the center of gravity of the "cloud" of migrating simulated fluid particles around Joukowsky profiles whose lift coefficient is known, and compares the theoretical lift coefficient with the numerically determined value of path deflection of the center of gravity, resulting from the random walk experiment. The theoretical discussion of the path deflection leads to a formula which predicts the maximum of possible C_f one can obtain with circulation around wing sections in ideal fluids.

1 INTRODUCTION

This paper deals with the analogy between fluid fronts migrating in filter paper and the hydrodynamic behavior of inviscid fluids [1], and the numerical fluid flow model of unsteady creeping flow, which allows to determine the lift coefficient of wing sections [2]. The "particles" in this "Random Walk Source Model" do not interact with each other as opposed to the cellular automaton methods, but local rules are set in such a way that the front of migrating "particles" carries the history of the average "particle" on its way to its place in the lattice. We will examine the center of gravity of a "particle cloud" on its path around a wing section.

2 THE RANDOM WALK SOURCE MODEL

2.1 Migration of fluid fronts in filter paper

When cutting the contour of a wing section from a sheet of filter paper, as is used in paper chromatography, and placing the leading edge of the paper into a liquid (e.g. water, Fig. 1) the liquid fronts are migrating through the paper. These fronts are separated at the wing section into a left and a right front. A cut in the paper (separation line) keeps the fronts separated after passing the wing section. The difference in migration length d , measured at the separation line, is proportional to the lift coefficient C_f of the wing section in potential flow [1]. $F_L = C_l \cdot \frac{\rho}{2} \cdot u_\infty^2 \cdot A$, F_L lift force, ρ mass density, u_∞ velocity, A wing area.

2.2 Two approaches will show that the difference in the migration of fluid fronts in filter paper around wing sections yields the lift coefficient [2]

It is possible to substitute the flow field (velocity u_∞ in infinity) around a wing section of the length T , with circulation Γ by a central vortex which has the same circulation Γ as the wing itself [3].

This vortex induces the velocity $w(\frac{T}{2})$ at the position of the trailing edge:

$$w(\frac{T}{2}) = \frac{\Gamma}{\pi T}$$

$$\Gamma = w(\frac{T}{2}) \cdot \pi \cdot T$$

$$C_l = \frac{2 \cdot \Gamma}{u_\infty \cdot T}$$

$$C_l = \frac{2 \cdot \pi \cdot w(\frac{T}{2})}{u_\infty}$$

where d is the migration difference of the fluid fronts in the direction of the separation line (Fig. 1)

$$\frac{w(\frac{T}{2})}{u_\infty} = \frac{d}{T}$$

$$C_l = 2 \cdot \pi \cdot \frac{d}{T}$$

Second approach:

Following a particle passing the wing section close to the wall, the path length of the average fluid particle around the left side is called s_o . The length of the path of the average fluid particle passing the right side is called s_u . Without circulation $s_o = s_u$. The time to pass the wing section is $t = \frac{T}{|u_\infty|}$.

In order to perform the Joukowsky rule we need to know the velocity $|u|$ at the edge of the wing section. This means that the fluid fronts have to reach the leading edge of the profile at the same time.

$$d = |u| \cdot t$$

$$d = |u| \cdot \frac{T}{|u_\infty|}$$

$$\frac{d}{T} = \frac{|u|}{|u_\infty|}$$

$$C_l = \frac{2 \cdot \Gamma}{T \cdot |u_\infty|}$$

$$C_l = 2 \cdot \pi \cdot \frac{d}{T}$$

2.3 Random Walk Source Model in analogy to potential flow

According to Darcy's law for fluid flow in porous media [4], the volume flux q per cross section is proportional to the negative of the mechanical potential gradient, of which only the pressure gradient ∇p is relevant in thin paper sheets, and is inversely proportional to the liquid's viscosity η . The proportionality constant is the permeability of the material to the liquid, k .

$$q = - \left(\frac{k}{\eta} \right) \cdot \nabla p$$

Continuum equations with pressure $p(x_1, x_2, x_3)$ leads to

$$\Delta p = \frac{\partial^2 p}{\partial x_1^2} + \frac{\partial^2 p}{\partial x_2^2} + \frac{\partial^2 p}{\partial x_3^2} = 0$$

analogous to

$$\Delta \Phi = \frac{\partial^2 \Phi}{\partial x_1^2} + \frac{\partial^2 \Phi}{\partial x_2^2} + \frac{\partial^2 \Phi}{\partial x_3^2} = 0$$

where Φ is the potential of the velocity vector field.

We introduce point sources at the leading edge of the paper in order to convert the migration of fluid fronts in filter paper, as shown in Fig. 1, into a model.

The distribution of the velocity in a source results from the displacement of particles coming out of the center. The following algorithm, which the author calls "Random Walk Source Model," is obtained by converting a source into a random walk model, without observing the detailed path of the particles that have left the center.

2.4 Description

A two-dimensional orthogonal lattice modeling fluid flow in the presence of obstacles, consists of cells $a_{i,j}$. Each cell can have three different values:

- $a_{i,j} = 1$: this cell has one particle,
- $a_{i,j} = 0$: this cell has no particle,
- $a_{i,j} = 2$: this cell cannot change its value: it cannot take a particle.

In the beginning, none of the cells have a particle. At the first time step, one cell acquires the value "1" (singularity of the source). This means that one particle has left the center of the source. At the second time step, the algorithm tests the value of one of the four neighboring cells in orthogonal direction selected at random. Three results are possible:

• Result 1: cell has the value "0." The algorithm changes the value to "1." This means that this cell now has a particle. The next particle starts in the singularity of the source at the next time step.

• Result 2: cell has the value "1," a particle is already present, test another randomly selected cell in orthogonal direction until you find a cell with the value "0." Proceed to result 1.

• Result 3: cell has the value "2," the tested cell cannot take a particle, test one of the three other possible neighboring cells and select one of them at random. Proceed to result 2.

This behavior can be viewed as the behavior of a fluid particle, starting from one source, and making a random walk to the region boundary. This boundary is formed by all particles that have previously left the source. The particle randomly touches the obstacles in the flow region, and settles down in the first free space near the boundary. The boundary is viewed as an equipotential line of unsteady potential fluid flow. Figs. 2 to 4 show the evolution of a "particle cloud" generated in the random walk source model.

3 NUMERICAL EXPERIMENTS REGARDING THE CENTER OF GRAVITY OF "PARTICLE CLOUDS" IN THE RANDOM WALK SOURCE MODEL

The approach to this problem is to simulate parallel flow with point sources. This is done by situating these sources on a line, which stands perpendicular to the flow direction, in front of the wing section (Fig. 5). Each particle comes out of one of several sources, the center of which is selected at random on the "source line." The boundary cells with the value "2" define the contour of the examined wing sections. The separation line at the trailing edge also consists of cells with the value "2," in order to keep the fronts separated (according to the Joukowski rule). While the "particle cloud" (all cells having a value of "1") is creeping into the direction of the wing section, the center of gravity of the "particle cloud" is plotted.

3.1 Expected deflection of the center of gravity of a "particle cloud" passing a wing section in the Random Walk Source Model

3.2 First approach, blade rows (Fig. 6)

$$\Gamma = (\vec{u}_{2e} - \vec{u}_{2a}) \cdot t$$

$$\vec{u}_{1e} = \vec{u}_{1a}$$

$$F_2 = \rho \cdot \vec{u}_e \cdot \Gamma \cdot b$$

$$\frac{\vec{u}_{2a}}{\vec{u}_a} = \sin \beta$$

$$\frac{\vec{u}_{2a}}{\vec{u}_e} = \sin \beta$$

$$\Gamma = -\vec{u}_e \cdot \sin \beta \cdot t$$

$$F_2 = C_a \cdot \frac{\rho}{2} \cdot |u_e|^2 \cdot b \cdot T$$

$$F_2 = \rho \cdot \vec{u}_e \cdot (-\vec{u}_e) \cdot \sin \beta \cdot t$$

$$C_l = \frac{\rho}{2} \cdot |\vec{u}_e|^2 \cdot b \cdot T = \rho \cdot |\vec{u}_e|^2 \cdot \sin \beta \cdot t$$

$$C_l = 2 \cdot \frac{t}{T} \cdot \sin \beta$$

3.3 Second approach, single blade (Fig. 7).

$$F = 2 \cdot \rho \cdot b \cdot t \cdot |\vec{u}_\infty|^2 \cdot \sin \frac{\beta}{2}$$

$$F_y = 2 \cdot \rho \cdot b \cdot t \cdot |\vec{u}_\infty|^2 \cdot \sin \frac{\beta}{2} \cdot \cos \frac{\beta}{2}$$

$$F_y = C_l \cdot \frac{\rho}{2} \cdot |\vec{u}_\infty|^2 \cdot A$$

$$2 \cdot \rho \cdot b \cdot t \cdot |\vec{u}_\infty|^2 \cdot \sin \frac{\beta}{2} \cdot \cos \frac{\beta}{2} = C_l \cdot \frac{\rho}{2} \cdot |\vec{u}_\infty|^2 \cdot A$$

$$C_l = 4 \cdot \frac{b \cdot t}{A} \cdot \sin \frac{\beta}{2} \cdot \cos \frac{\beta}{2}$$

$$\sin \frac{\beta}{2} \cdot \cos \frac{\beta}{2} = \frac{1}{2} \cdot \sin \beta$$

$$C_l = 2 \cdot \frac{b \cdot t}{A} \cdot \sin \beta$$

$$\frac{b \cdot t}{A} = \frac{t}{T}$$

$$C_l = 2 \cdot \frac{t}{T} \cdot \sin \beta$$

3.4 Third approach, volume flux close to the blade (Fig- 8)

$$F = \rho \cdot \dot{V} \cdot \vec{u}_T$$

$$F = C_l \cdot \frac{\rho}{2} \cdot |\vec{u}_\infty|^2 \cdot A$$

$$C_l = \frac{2 \cdot F}{\rho \cdot |\vec{u}_\infty|^2 \cdot A} = \frac{2 \cdot \rho \cdot \dot{V} \cdot \vec{u}_T}{\rho \cdot |\vec{u}_\infty|^2 \cdot A}$$

$$C_l = \frac{2 \cdot \dot{V}}{B \cdot T \cdot |\vec{u}_\infty|} \cdot \frac{|\vec{u}_T|}{|\vec{u}_\infty|}$$

$$\frac{|\vec{u}_T|}{|\vec{u}_\infty|} = \sin \beta, \dot{V} = t \cdot b \cdot |\vec{u}_\infty|$$

$$C_l = 2 \cdot \frac{t}{T} \cdot \sin \beta$$

3.5 C_f and von Karman vortex street

The unknown parameter in the formula concerning C_f is t .

Supposition: view the wing section blade row as a generator of a von Karman vortex street by starting and stopping the blade row once. (Fig. 9):

$$\frac{\vec{u}_T}{\vec{u}_\infty} = \sin \beta, \text{ where}$$

$$\vec{u}_T = \frac{\Gamma}{2l} \cdot \tanh\left(\pi \cdot \frac{h}{l}\right) \text{ von Karman.}$$

$$\frac{\frac{\Gamma}{2l} \cdot \tanh\left(\pi \cdot \frac{h}{l}\right)}{\vec{u}_\infty} = \sin \beta$$

$$\Gamma = \frac{C_l \cdot T \cdot |\vec{u}_\infty|}{2}$$

$$\frac{C_l \cdot \tanh\left(\pi \cdot \frac{h}{l}\right) \cdot T \cdot |\vec{u}_\infty|}{2 \cdot 2 \cdot l \cdot |\vec{u}_\infty|} = \sin \beta,$$

$$\frac{1}{2} \tanh\left(\pi \cdot \frac{h}{l}\right) = \frac{1}{\sqrt{8}}, \text{ von Karman}$$

$$\frac{C_l \cdot T}{2 \cdot \sqrt{8}} \cdot \frac{T}{l} = \sin \beta$$

Supposition: $\frac{T}{l} = 0,281 = \frac{h}{l}$,

$$C_l = \frac{2 \cdot \sqrt{8}}{0,281} \cdot \sin \beta$$

This formula leads to a maximum possible C_f if $\sin \beta=1$

$$C_{l(\sin \beta=1)} = \frac{2 \cdot \sqrt{8}}{0,281} \cdot \sin \beta = 20.163 \dots$$

4 COMPARISON OF THEORETICAL APPROACH TO EXPERIMENTAL DATA IN THE RANDOM WALK SOURCE MODEL

Figs. 10 to 15 show the expected deflection of the path of the center of gravity from a "particle cloud" as it creeps around a wing section in the Random Walk Source Model (theoretically determined gradient shown as line with angle β), compared to the experimental results. The path of the center of gravity is shown as dotted line.

4.1 Discussion

The author has used a random walk algorithm for fluid flow in unsteady potential flow by analyzing creeping flow in porous media. The model differs from other cellular automaton methods [6] because particles do not collide with each other, but local rules are set in such a way, that the front of migrating particles carries the history of an average particle on its way in the lattice. Simulating a fluid flow around wing sections while plotting the center of gravity of the "particle cloud" and the theoretical discussion of this model leads to the formula $C_l = \frac{2 \cdot \sqrt{8}}{0,281}$ by using a blade row as generator for a von Karman vortex street, which implies the result, that the maximum theoretical C_f generated by circulation is $C_{l(\sin \beta=1)} = \frac{2 \cdot \sqrt{8}}{0,281} \cdot \sin \beta = 20.163 \dots$

References

1. R. Meyer, Neue Methode zur Ca- und Cw-Wert Bestimmung von Tragflugelprofilen bei Potentialströmung, Bundeswettbewerb Jugend forscht, Berlin [1980].
2. R. Meyer, Random walks and hydrodynamical lift from wing sections, Physica A 242(1997)230-238
3. J.H. Spurk, Strömungslehre, Springer Verlag, Berlin, 1993
4. H. Darcy, Les fontaines publiques de la ville de Dijon, Paris, 1856
5. E. Trefftz, Vgl. Z. Flugtechnik (1913) S.130
6. U. Frisch, B. Hasslacher and Y. Pomeau, Lattice gas automata for Navier-Stokes equations, Phys. Rev. Lett. 56,1505 (1986)

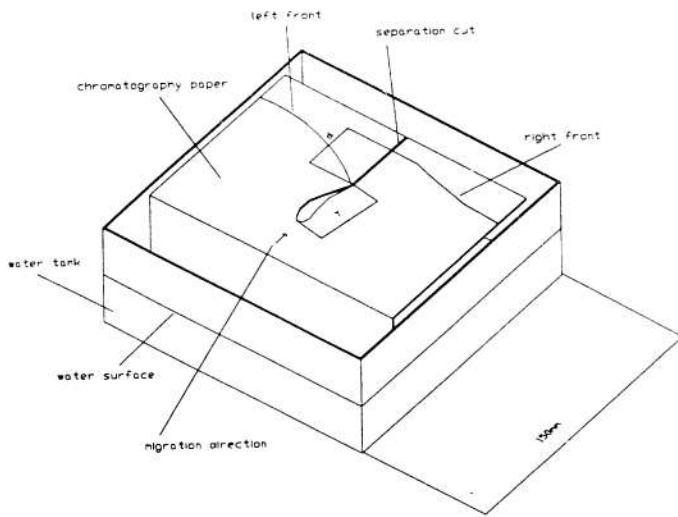


Fig. 1: Migration of fluid fronts in filter paper, the difference in migration length d of left and right front is proportional to the lift coefficient of the wing section [1].

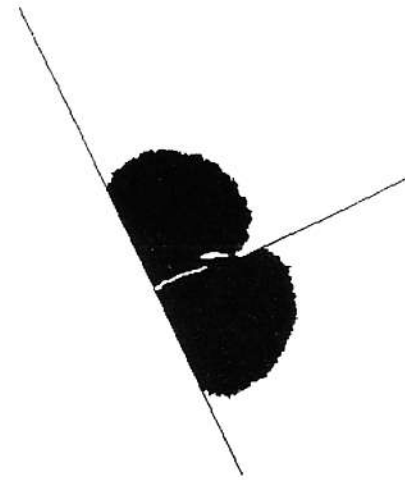


Figure 4

Figs. 2 to 4: Growing "particle cloud" generated using the random walk source model creeping around a wing section center of gravity of the "cloud" is plotted as path during creeping.

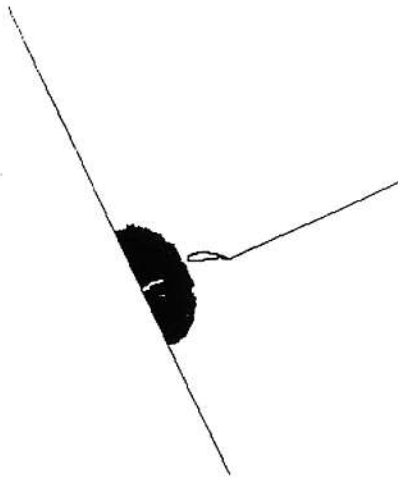


Figure 2

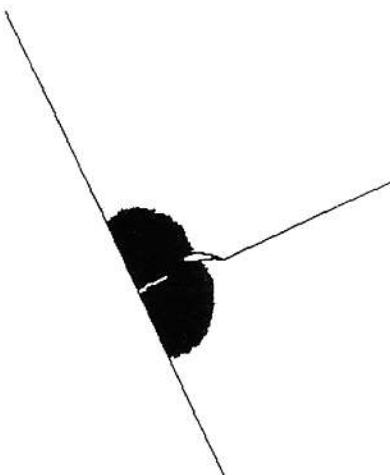


Figure 3

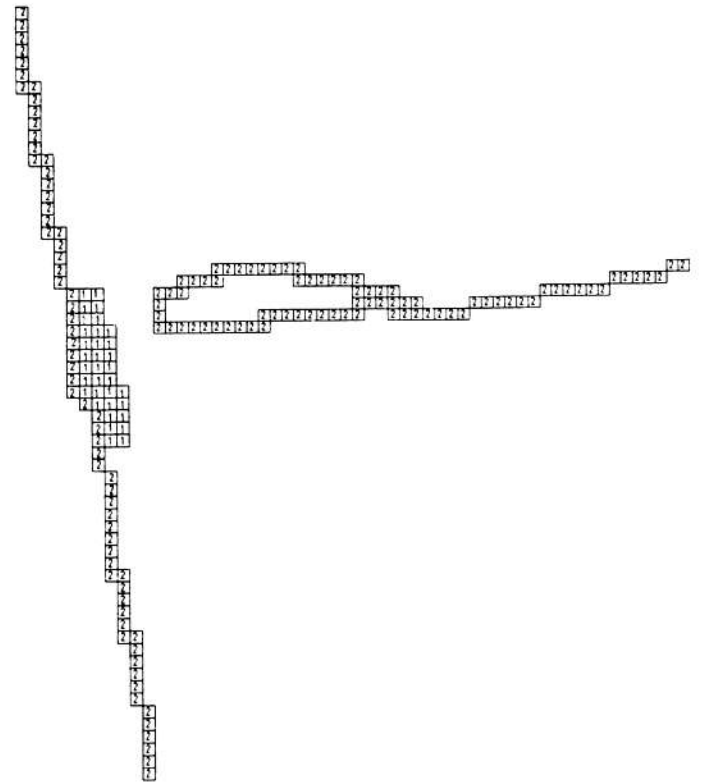


Fig. 5: Simulated fluid flow around an obstacle, showing that each cell can have three values:

- "1" cell has one particle,
- "0" this cell has no particle,
- "2" this cell cannot take a particle and cannot become occupied.

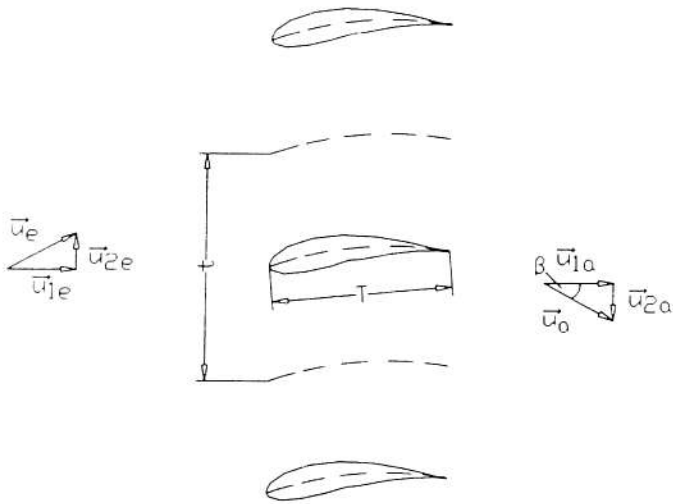


Fig. 6: Applying the equation of momentum for ideal fluids in blade rows leads to

$$C_l = \frac{2t}{T} \cdot \sin \beta$$

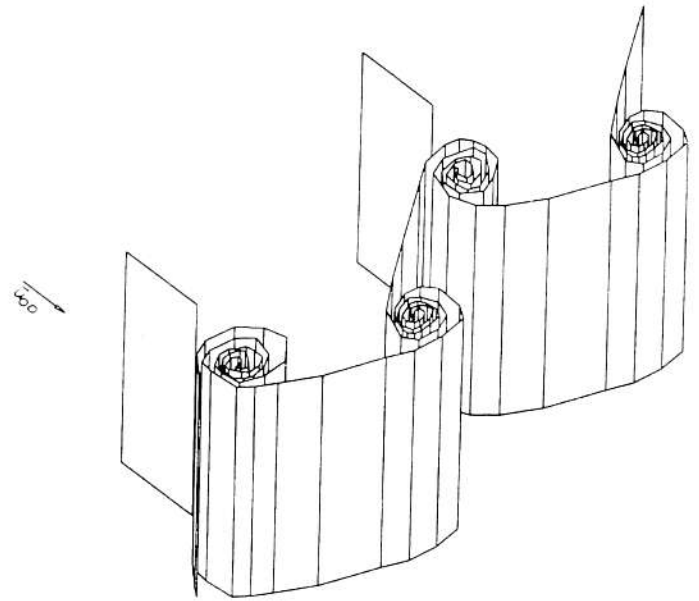


Fig. 9: Blade row start and stop flow generates von Karman vortex street.

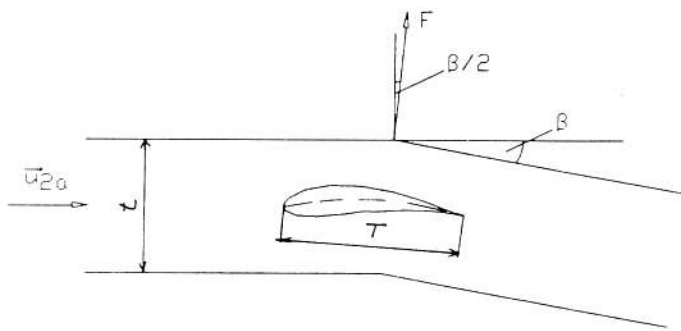


Fig. 7: Applying the equation of momentum for ideal fluids free surface jet around a wing section leads to $C_l = \frac{2t}{T} \cdot \sin \beta$

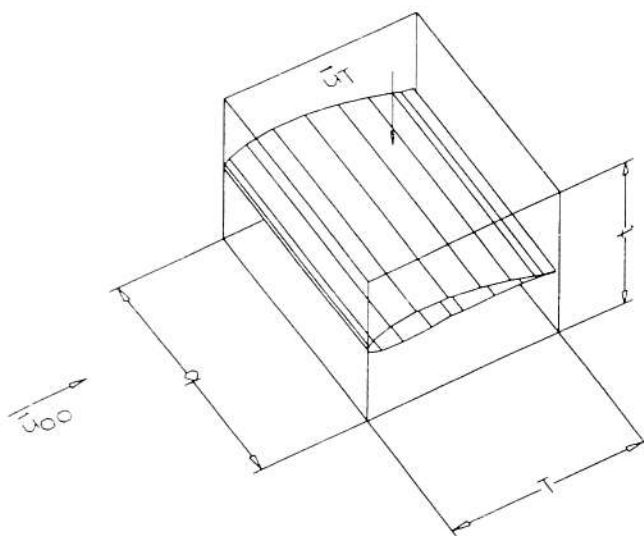


Fig. 8: Applying the volume flux close to a wing section leads to $C_f = \frac{2t}{T} \cdot \sin \beta$

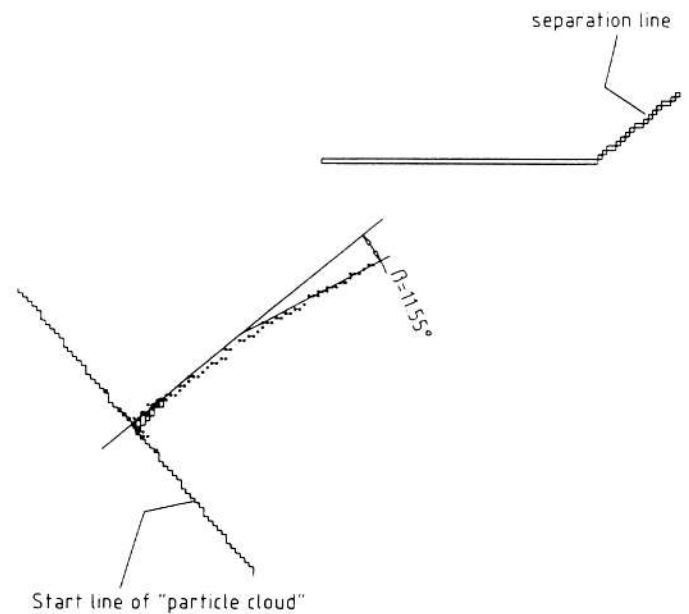


Fig. 10: Center of gravity of a "particle cloud" generated in the random walk source model, creeping around a wing section. Wing section is result of a conformal plot (Joukowski plot[5]). Center of conformal plotted circle $x_0 = 0, y_0 = 15$, angle of attack $\alpha = 40^\circ$.

Proposed definition: $C_l = 20.163... \cdot \sin \beta$. Obtained by comparing the expected gradient of the deflected path of the center of gravity of the "particle cloud" when the slower front has reached the trailing edge of the wing section shown as line, to the experimental result of path plotting shown as dotted line.

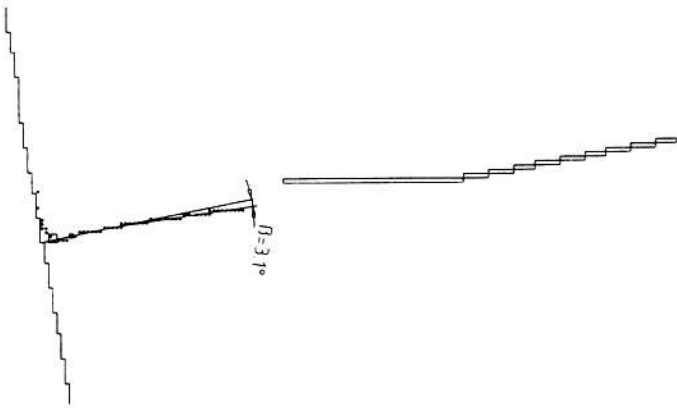


Fig. 11: Center of gravity of a "particle cloud" generated in the random walk source model, creeping around a wing section is the result of a conformal plot (Joukowski plot). Center of conformal plotted circle : $x_0 = 0, y_0 = 0, a = 10$, angle of attack $\alpha = 10^\circ$.

Proposed definition: $C_f = 20.163... - \sin \beta$. Obtained by comparing the expected gradient of the deflected path of the center of gravity of the "particle cloud" when the slower front has reached the trailing edge of the wing section shown as line, to the experimental result of path plotting shown as dotted line.

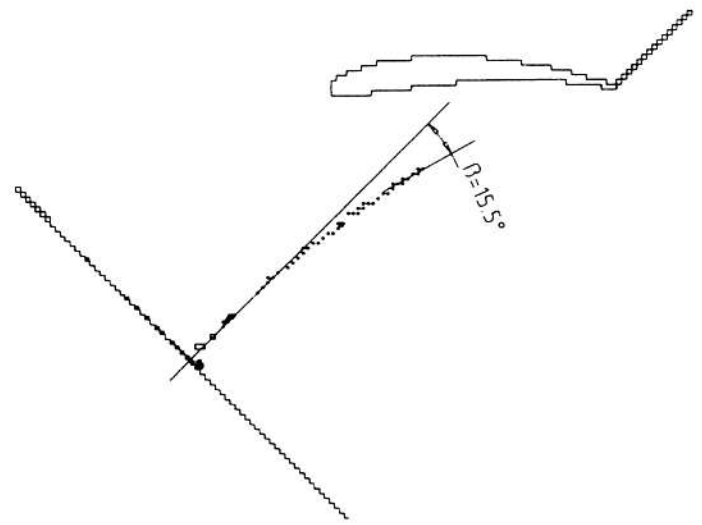


Fig. 13: Center of gravity of a "particle cloud" generated in the random walk source model, creeping around a wing section. Wing section is result of a conformal plot (Joukowski plot)

Center of conformal plotted circle
 $x_0 = -1, y_0 = 2, a = 15$, angle of attack $\alpha = 45^\circ$.

Proposed definition: $C_f = 20.163... \sin \beta$. Obtained by comparing the expected gradient of the deflected path of the center of gravity of the "particle cloud" when the slower front has reached the trailing edge of the wing section shown as line, to the experimental result of path plotting shown as dotted line.

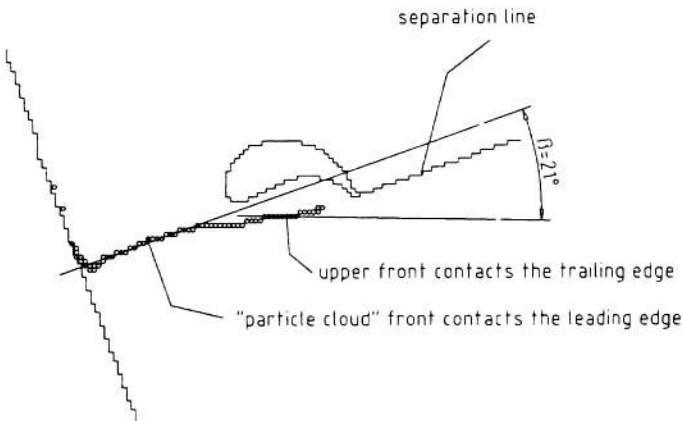


Fig. 12: Center of gravity of a "particle cloud" generated in the random walk source model, creeping around a wing section. Wing section is result of a conformal plot (Joukowski plot). Center of conformal plotted circle

$x_0 = -2, y_0 = 5, a = 10$, angle of attack $\alpha = 20^\circ$.

Proposed definition: $C_f = 20.163... - \sin \beta$. Obtained by comparing the expected gradient of the deflected path of the center of gravity of the "particle cloud" when the slower front has reached the trailing edge of the wing section shown as line, to the experimental result of path plotting shown as dotted line.